PHYSICAL REVIEW B VOLUME 47, NUMBER 9 1 MARCH 1993-I

ac susceptibilities of a network of resistively shunted Josephson junctions with self-inductances

T. Wolf
Fakultät für Physik, Universität Konstanz, D-7750 Konstanz, Germany

A. Majhofer
Institute of Experimental Physics, Warsaw University, PL-00 681 Warsaw, ul. Hoza 69, Poland
(Received 13 July 1992; revised manuscript received 19 October 1992)

We investigate the magnetic response of a two-dimensional system of resistively shunted Josephson junctions to dc and ac magnetic fields. Treating screening effects self-consistently we obtain hysteresis curves, ac susceptibilities, and higher harmonics of magnetization that are very similar to experimental observations on high-T_c superconductors.

I. INTRODUCTION

Ceramic samples of high-T_c superconductors generally show irreversible magnetic effects, which were attributed by Takashige, Bednorz, and Müller[1] to the existence of tunneling junctions between superconducting grains. Since then, networks of Josephson junctions have been widely used to model magnetic properties[2–7] and current-voltage characteristics[8,9] of these materials. The applicability of this model has been extended to crystallite and single-crystal samples following the argument of Deutscher and Müller[10] that due to a very short coherence length in high-T_c superconductors, twinning planes, faults in stoichiometry, and other defects act like intrinsic weak links between domains characterized by well-defined phases of the order parameter. A positionally disordered system of Josephson junctions may thus be regarded as a limiting case of a strongly disordered, inhomogeneous superconductor.[11,12] Intensive numerical simulations[2–9] of such systems have indeed reproduced many aspects of the physics of high-T_c superconductors and were instrumental in investigating such concepts as "superconducting glass state"[2–4] and "vortex glass."[5–7]

The usual approximation mostly assumed in the work mentioned was to neglect magnetic fields produced by the superconducting currents induced in the system. On the other hand, flux movement in high-T_c superconductors subject to an external ac field[13,14] was successfully described within the critical-state model developed for conventional hard superconductors.[15,16] Similarly, the flux-creep model[17] has been applied to explain the logarithmic time decay of the remanent magnetization in the high-T_c materials.[18] In both of these cases local screening currents induced in a superconductor determine the observed magnetic response.

In our previous work[19] we have shown that these views of strongly inhomogeneous superconductors may be combined if one takes into account screening effects in a Josephson-network model. We investigated a two-dimensional lattice of superconducting grains with nearest-neighbor grains coupled via Josephson junctions. The magnetic flux through each mesh was put equal to the sum of the external flux and the flux of the field produced by the induced currents, which was approximately taken as proportional to the current around the mesh. We have shown that within such a simple model it is possible to reproduce a wide spectrum of magnetic properties ranging from a vortex lattice to spatial magnetization patterns similar to the Bean model.[15]

In this paper we extend our model to disordered lattices and allow for the dependence of the critical current through each junction on the local magnetic field. Solving the overdamped equations of motion, we calculate hysteresis curves and ac susceptibilities of the system. Due to the nonlinearity of the equations of motion, higher harmonics of the driving ac field are also present in the magnetic response. Measurements of higher harmonics of the ac susceptibility have been used to investigate conventional composite, layered, and granular superconducting materials.[20] For high-T_c superconductors the existing data on higher harmonics is usually interpreted within the critical-state model[13,14,21] or by modeling the sample as an ensemble of independent loops with one weak link.[22–24] Here, we are in principle able to relate the measured ac susceptibilities and their higher harmonics to such intrinsic properties of the material as characteristic grain sizes and coupling strengths of the links. We therefore conclude our paper with a short discussion of the values of parameters which one should take to make our comparison with experimental results quantitative. The last point is the subject of further investigation.

II. MODEL

We consider a system of superconducting grains placed on a two-dimensional lattice. Each grain is coupled via Josephson junctions with its four nearest neighbors [see Fig. 1(a)]. Generally, each junction may be characterized by its maximal superconducting current I_0, its normal resistance R, its capacitance C, and the gauge-invariant phase difference Θ,

$$\Theta=\Delta\varphi-\frac{1}{\phi_0}\int \mathbf{A}\cdot d\mathbf{l} , \qquad (1)$$

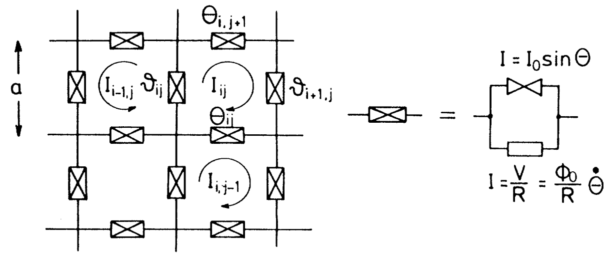

(a)

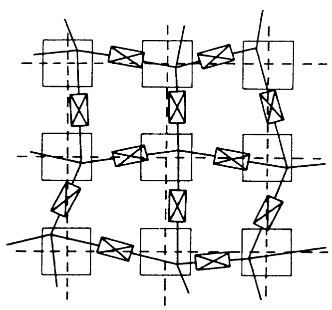

(b)

FIG. 1. (a) A schematic view of a network of weak links used as a model of an inhomogeneous superconducting medium. (b) Disordered network, generated from that of (a) by randomly choosing new positions of the nodes within a square of side $a/2$.

where $\Delta\varphi$ is the difference in phases of superconducting order parameters in grains forming the link, $\phi_0=\Phi_0/2\pi$ with the elementary flux quantum $\Phi_0=h/2e$, $\mathbf{A}$ is the vector potential, and the integral is taken across the junction. To describe the whole system we introduce "horizontal" and "vertical" gauge-invariant phase differences $\vartheta_{i,j}$ and $\Theta_{i,j}$, respectively, and, in the absence of external currents, describe all possible currents as superpositions of elementary circular currents $I_{i,j}$ [see Fig. 1(a)]. Since we are interested in slow processes we turn to the overdamped (zero capacitance) limit and obtain

$$I_{i,j}-I_{i,j+1}=I_0\sin\Theta_{i,j+1}+\frac{\phi_0}{R}\frac{d\Theta_{i,j+1}}{dt}\ , \tag{2}$$

$$I_{i,j}-I_{i-1,j}=I_0\sin\vartheta_{i,j}+\frac{\phi_0}{R}\frac{d\vartheta_{i,j}}{dt}\ . \tag{3}$$

As in the previous paper[19] we consider here only zero-field-cooled samples at temperatures below the superconducting transition of the grains. In this case the magnetic flux $\phi_{i,j}$ through a single mesh (i,j) is given by[25]

$$\frac{\phi_{i,j}}{\phi_0}=\vartheta_{i,j}+\Theta_{i,j+1}-\vartheta_{i+1,j}-\Theta_{i,j}\ . \tag{4}$$

Generally $\phi_{i,j}$ depends linearly on the external field (or corresponding flux $\phi_{i,j}^{\text{ext}}$), the current $I_{i,j}$ and all other currents in the network. As in our previous work we adopt the local approximation, putting

$$\phi_{i,j}=\phi_{i,j}^{\text{ext}}-LI_{i,j}\ . \tag{5}$$

A continuous version of the system described by Eqs. (2)–(5) is equivalent to the "Josephson medium" as considered by Sonin[26] and Sonin and Tagantsev.[27] Given $\phi_{i,j}^{\text{ext}}$, Eqs. (2)–(5) are easily reduced to a system of coupled ordinary differential equations for $\Theta_{i,j}$ and $\vartheta_{i,j}$ only. In the previous work[19] we considered a regular square lattice and hence took $\phi_{i,j}^{\text{ext}}=H_{\text{ext}}S$ where H_{ext} is the external field and S, the area of a single plaquette.

Here, two extensions are made. First we introduce disorder into our lattice. To generate disordered networks we start with a regular square lattice with lattice constant a and then randomly choose a new position of each lattice point within a square of side $a/2$ centered on the regular position with its sides parallel to the starting regular lattice. This construction is schematically depicted in Fig. 1(b). Therefore we have

$$\phi_{i,j}^{\text{ext}}=H_{\text{ext}}S_{i,j}\ , \tag{6}$$

where $S_{i,j}$, the area of a mesh (i,j). Second, we allow for the dependence of I_0 on the local magnetic field H_{loc} taken as an average of the values in the adjacent plaquettes. For the horizontal link described by $\Theta_{i,j}$, H_{loc} is thus given by

$$H_{\text{loc}}=\frac{1}{2}\left[\frac{\phi_{i,j}}{S_{i,j}}+\frac{\phi_{i,j-1}}{S_{i,j-1}}\right] \tag{7}$$

and by a similar expression for $\vartheta_{i,j}$. With assumptions specified in Eqs. (6) and (7) we obtain the following system of equations:

$$\frac{d\vartheta_{i,j}}{dt}=\frac{R}{L}\left[\vartheta_{i-1,j}-2\vartheta_{i,j}+\vartheta_{i+1,j}+\Theta_{i,j}-\Theta_{i-1,j}+\Theta_{i-1,j+1}-\Theta_{i,j+1}+\left[\frac{\phi_{i,j}^{\text{ext}}}{\phi_0}-\frac{\phi_{i-1,j}^{\text{ext}}}{\phi_0}\right]-\beta\sin\vartheta_{i,j}\right]\ , \tag{8}$$

$$\frac{d\Theta_{i,j}}{dt}=\frac{R}{L}\left[\Theta_{i,j+1}-2\Theta_{i,j}+\Theta_{i,j-1}+\vartheta_{i,j}-\vartheta_{i,j-1}+\vartheta_{i+1,j-1}-\vartheta_{i+1,j}+\left[\frac{\phi_{i,j-1}^{\text{ext}}}{\phi_0}-\frac{\phi_{i,j}^{\text{ext}}}{\phi_0}\right]-\beta\sin\Theta_{i,j}\right]\ , \tag{9}$$

where $\beta=\beta(H_{\rm loc})=LI_0(H_{\rm loc})/\phi_0$. The necessary boundary conditions follow from Eqs. (2)–(5) when $I_{i,j}=0$ everywhere outside the system:

$$\frac{d\vartheta_{1,j}}{dt}=\frac{R}{L}\left[\frac{\phi_{1,j}^{\rm ext}}{\phi_0}-\vartheta_{1,j}+\vartheta_{2j}-\Theta_{1,j+1}+\Theta_{1,j}-\beta\sin\vartheta_{1,j}\right], \quad (10)$$

$$\frac{d\Theta_{i,1}}{dt}=\frac{R}{L}\left[-\frac{\phi_{i,1}^{\rm ext}}{\phi_0}+\Theta_{i,2}-\Theta_{i,1}+\vartheta_{i,1}-\vartheta_{i+1,1}-\beta\sin\Theta_{i,1}\right]. \quad (11)$$

Analogous conditions hold for the remaining two edges of the network. Equations (8)–(11) are solved numerically for different forms of $\beta(H_{\rm loc})$ and the external field of the form

$$H_{\rm ext}(t)=H_{\rm dc}+H_{\rm ac}\cos(\omega t)\ . \quad (12)$$

Local magnetic fluxes and the time-dependent magnetization $M(t)$ of the system, defined as

$$M(t)=\frac{1}{N^2}\sum_{i,j}[\phi_{i,j}(t)-\phi_{i,j}^{\rm ext}(t)] \quad (13)$$

(where N^2 is the total number of plaquettes in the system) are then calculated using Eq. (4). If the sweep of the field is slow enough, steady oscillations are induced in the system and, after some transient time, $M(t)$ is a periodic function of time with period $2\pi/\omega$. It may thus be expanded as a Fourier series,

$$M(t)=H_{\rm ac}\sum_{n=0}^{\infty}[\chi_n'\cos(n\omega t)+\chi_n''\sin(n\omega t)]\ . \quad (14)$$

The quantities χ_n' and χ_n'' are the real and imaginary parts of the susceptibility χ_n.

III. RESULTS AND DISCUSSION

Before coming to more realistic calculations within a model containing both positional disorder and field-dependent I_0, we first discuss the role of the two factors separately. Figure 2(a) shows a hysteresis curve for a regular system (i.e., regular, square lattice) of 30×30 junctions with $\beta=5$ (and field-independent), $H_{\rm dc}=0$, $H_{\rm ac}=100\phi_0/a^2$ (a is the lattice constant), and the ac-field frequency $\omega=4\times10^{-4}\ R/L$. Spatial distribution of the flux within the system for the conditions specified above is similar to that predicted by the Bean model[15] of hard superconductors (cf. Ref. 19). Since the equations of motion [Eqs. (8)–(11)] contain nonlinear terms, higher harmonics of the ac-field frequency are also present in the magnetic response. Their real and imaginary parts χ_n' and χ_n'' can easily be measured in real experiments or numerical simulations and give more precise information about the system than a hysteresis curve alone. The spectrum of the magnetic response corresponding to the hysteresis curve of Fig. 2(a) is shown in Fig. 2(b). For $H_{\rm dc}=0$ the hysteresis curve [Fig. 2(a)] is point symmetric with the origin as the center of symmetry [i.e., $M(H_{\rm ext})=-M(-H_{\rm ext})$], therefore all even-order harmonics in the spectrum of Fig. 2(b) are exactly zero ($|\chi_{2n}|=0$ for all n). In general, this symmetry disappears with $H_{\rm dc}\neq0$ and the even-order harmonics show up.

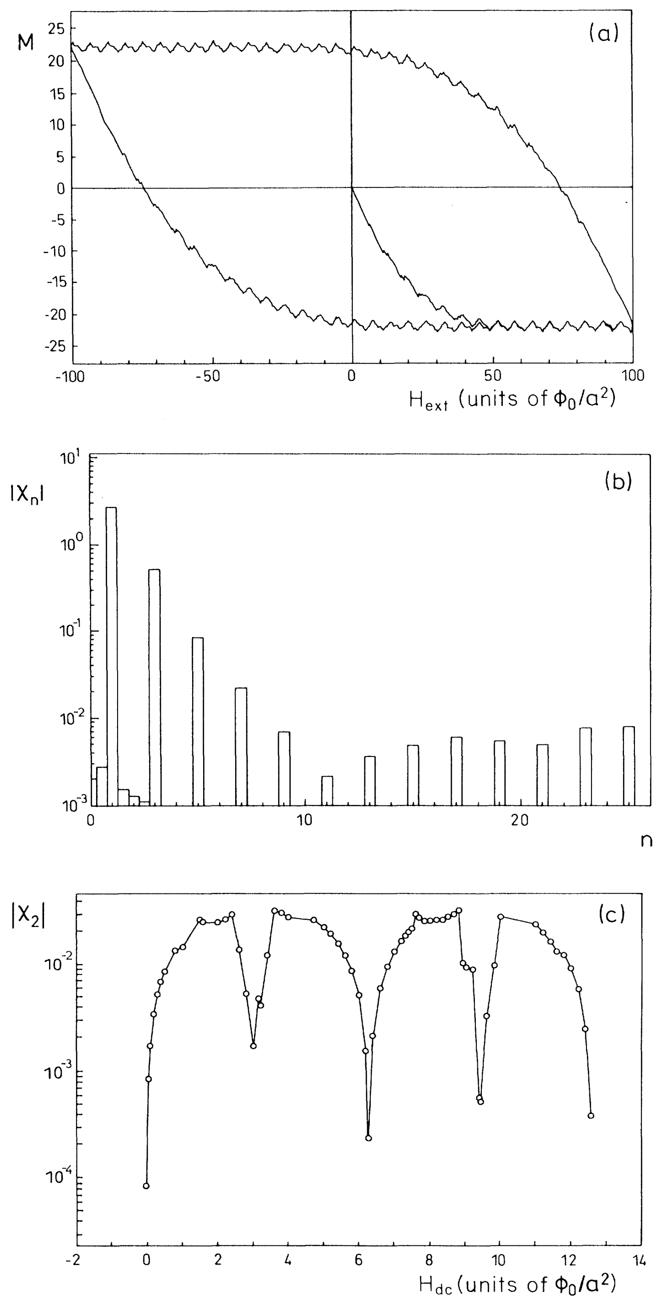

FIG. 2. Magnetization of a regular square lattice of 30×30 Josephson junctions for constant $\beta=5$. (a) The hysteresis curve for $H_{\rm dc}=0$, $H_{\rm ac}=100\phi_0/a^2$, and $\omega=4\times10^{-4}R/L$. (b) The spectrum of the magnetic response corresponding to the same conditions as in (a). (c) The absolute value of the second harmonic $|\chi_2|=\sqrt{\chi_2'^2+\chi_2''^2}$ as a function of the external dc field $H_{\rm dc}$; other conditions as in (a).

Within the Bean model, however, also for $H_{dc} \neq 0$ no even harmonics are generated. With $H_{dc} \neq 0$ the Josephson network discussed here predicts small, nonzero values of even-order harmonics for field-independent local critical currents [i.e., $\beta(H_{loc})=\text{const}$] although the corresponding spatial-flux distributions are in this case similar to the ones given by the Bean model. This is a clear indication that the calculated magnetic states of our model are not just "critical states," but more complicated ones. As an example Fig. 2(c) displays the absolute value of the second harmonic $|\chi_2| = \sqrt{\chi_2'^2 + \chi_2''^2}$ as a function of H_{dc} for a regular lattice of 30×30 Josephson junctions with $\beta = 5$. The characteristic periodic structure there results from the exact periodicity of the lattice and is not changed when the fixed value of β is replaced by some distribution around its mean value, although some features of $|\chi_2(H_{dc})|$ are then smoothed out. For a positionally disordered lattice, the additional periodic structure superimposed on the hysteresis curve disappears as seen in Fig. 3(a) [cf. Fig. 2(a)]. There we present an example of a hysteresis curve for a system of 30×30 junctions forming a disordered lattice [see Fig. 1(b)]. It is interesting to note here, that positional disorder strongly affects the spatial distribution of the remanent flux and in weak fields causes some local magnetic moments (fluxes) to assume a polarity antiparallel to the instantaneous direction of the external field. Such a possibility has al-

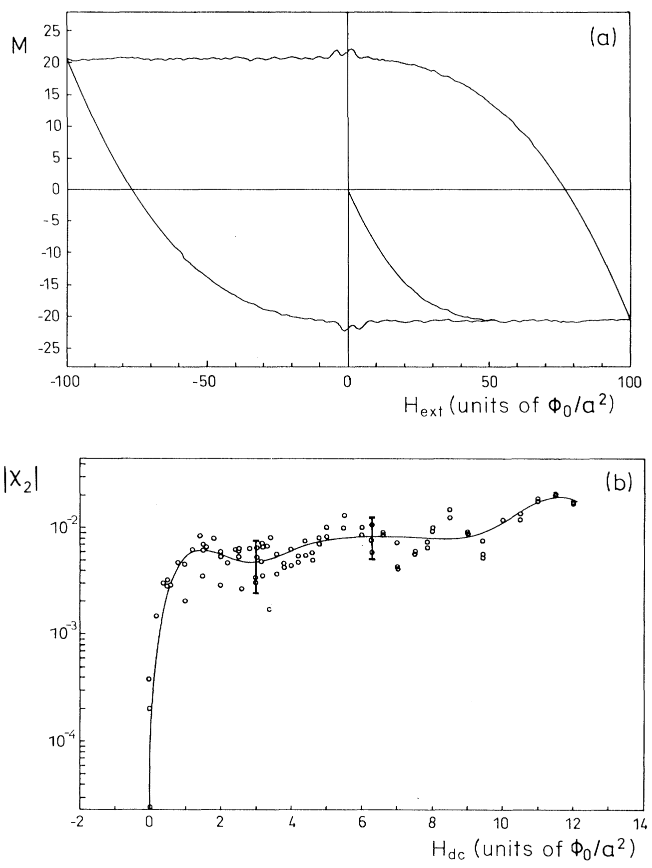

FIG. 3. Magnetization of a positionally disordered system of 30×30 Josephson junctions for constant value of $\beta = 5$. (a) The hysteresis curve for $H_{dc}=0$, $H_{ac}=100\phi_0/a^2$, and $\omega = 4 \times 10^{-4} R/L$. (b) The absolute value of the second harmonic $|\chi_2|$ as a function of the external dc field H_{dc}; and other conditions as in (a). Results computed for different statistically independent realizations of the disordered lattice (circles); and the fitted 10th-order polynomial (continuous line).

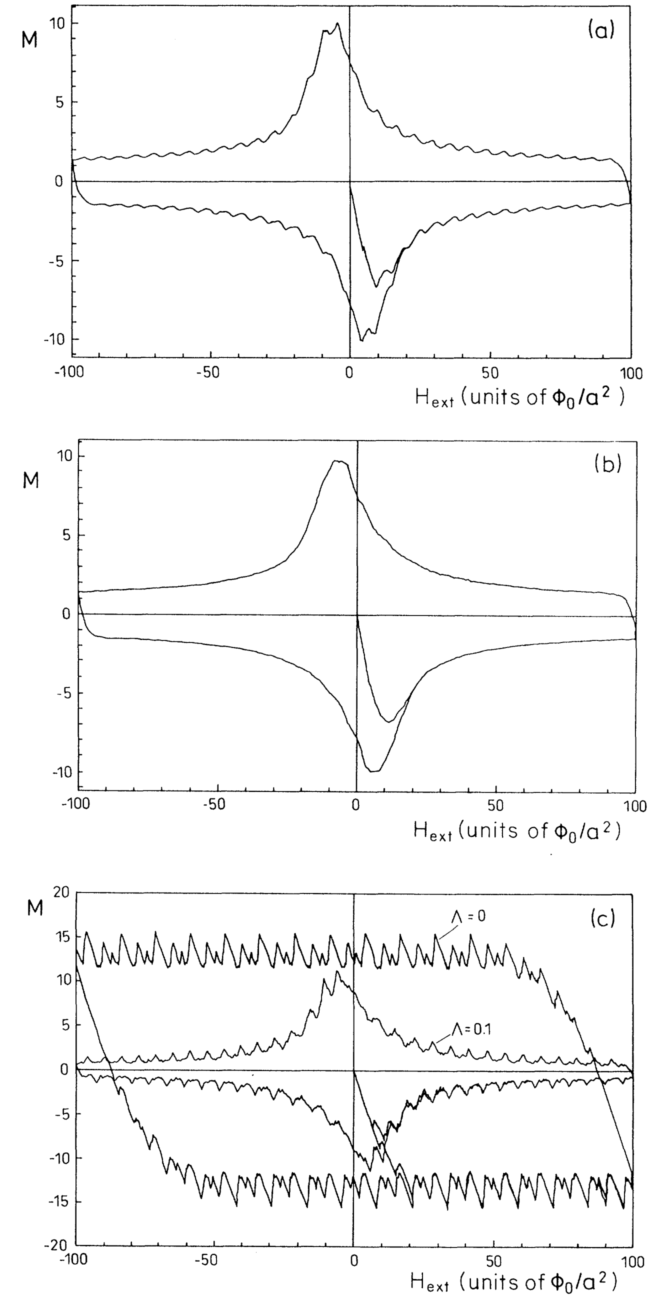

FIG. 4. The hysteresis curve for the system with field-dependent critical currents: $\beta(H_{loc}) = 5/(1+0.2|H_{loc}|)$, $\omega = 4 \times 10^{-4} R/L$, and $H_{dc}=0$ for (a) a regular square lattice of 30×30 junctions; (b) a positionally disordered system with 30×30 junctions; (c) a regular lattice of 10×10 junctions and different values of Λ.

ready been discussed by Malozemoff *et al.*[28] (cf. also Ref. 4). The periodicity of $|\chi_2|$ versus H_{dc} disappears for a disordered lattice. Except for the minimum at $H_{dc}=0$ all other sharp minima disappear and the value of $|\chi_2|$ increases slightly for large H_{dc} as shown in Fig. 3(b). Each point in Fig. 3(b) represents the result for one particular realization of the disordered lattice and the continuous line the 10th-order polynomial fitted to these points. The error bars indicate the deviations of the data points from the smooth curve, and are representative of the fluctuations due to disorder.

Measurements on ceramic samples show that $|\chi_2|$ first increases and then, after reaching its maximum value, decreases smoothly with increasing dc field. This was attributed[22–24,29] to the dependence of the critical current through a single junction on the value of the magnetic field. We followed this argument here. Numerical simulations indicate that assuming in our model the form of $\beta(H_{loc})$ as given by the Kim model[16,30]

$$\beta(H_{loc})=\frac{\beta_0}{1+\Lambda|H_{loc}|} \tag{15}$$

it is possible to obtain a magnetic response similar to that in the more exact model in which $I_0(H_{loc})$ of each link is taken as for the square Josephson junction of area s (cf. Ref. 25)

$$I_0(H_{loc})=I_0(0)\frac{|\sin(x)|}{|x|} \tag{16}$$

with $x=sH_{loc}/2\phi_0$ and normally distributed junction areas s.[31] In the following we therefore assume the simpler form given by Eq. (15). Figure 4(a) shows a hysteresis curve obtained for the regular system of 30×30 junctions with $\beta_0=5$, $H_{dc}=0$, and $\Lambda=0.2$. Additional small amplitude oscillations appear, again as a result of the regularity of the lattice. In Fig. 4(b) we show the hysteresis loop for one example of a disordered system of 30×30 junctions with $\Lambda=0.2$ and $H_{dc}=0$, $H_{ac}=100$. With increasing Λ more flux enters the system and its magnetization is reduced, as may be seen in Fig. 4(c) where hysteresis curves for a regular lattice of 10×10 junctions for $H_{dc}=0$ and two values of Λ are shown. A comparison of Figs. 2(a), 4(a), and 4(c) show that the amplitude of the oscillations caused by the periodicity of the lattice decreases with the size of the system.

With $\beta(H_{loc})$ given by Eq. (15) the amplitude of χ_2 de-

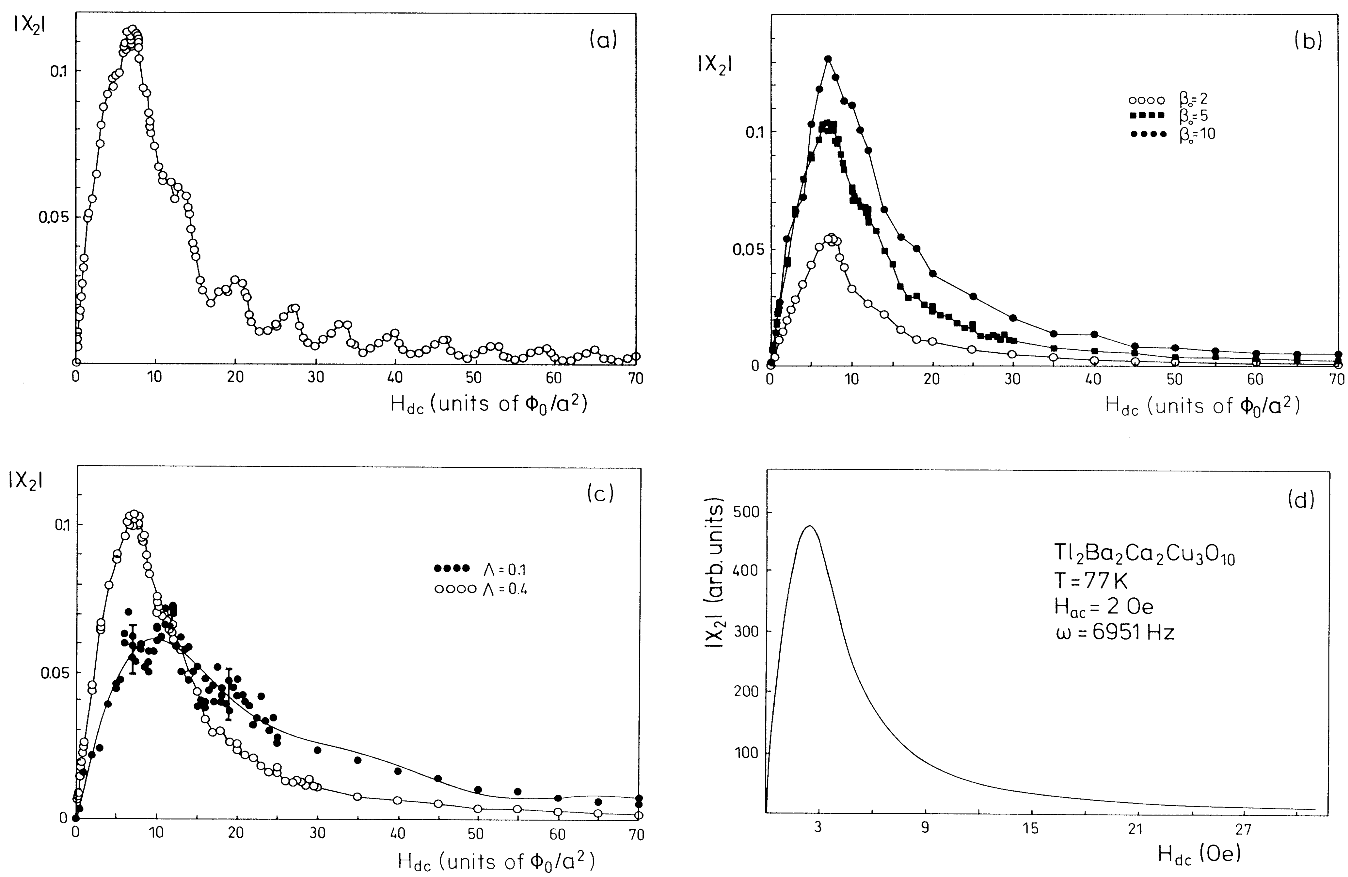

FIG. 5. $|\chi_2|$ as a function of the external dc field for a system of 10×10 junctions with $\beta(H_{loc})=\beta_0/(1+\Lambda|H_{loc}|)$, $\omega=2\pi\times10^{-3}R/L$, $H_{ac}=10\phi_0/a^2$, for (a) a regular square lattice with $\beta_0=5$, $\Lambda=0.4$; (b) a positionally disordered lattice, $\Lambda=0.4$ and different values of β_0; (c) a positionally disordered lattice, $\beta_0=5$ and different values of Λ; and (d) $|\chi_2|$ as a function of the external dc field measured on a $Tl_2Ba_2Cu_3O_{10}$ ceramic sample with $H_{ac}=2$ Oe, frequency $\omega=6951$ Hz (Ref. 32). In (b) and (c) each point represents the result for one independently constructed disordered lattice.

creases for large H_{dc} fields as displayed in Fig. 5(a), but for a regular system the additional periodic structure still remains. It disappears in the case of disordered lattice [Fig. 5(b)].

A realistic model must contain a built-in positional disorder and is characterized by two parameters β_0 and Λ. In Fig. 5(b) we show $|\chi_2|$ as a function of H_{dc} for a disordered system with $\Lambda=0.4$ and different values of β_0. For increasing β_0, the peak height grows, whereas the peak position remains unchanged. The values of β_0 taken to obtain curves shown in Fig. 5(b) lie within the realistic limits for ceramic samples estimated independently from the data on grain sizes and critical currents (cf. the discussion at the end of this section). In part (c) of Fig. 5, the same quantities as in Fig. 5(b) are shown for $\beta_0=5$ and different values of Λ. With increasing Λ, the peak position shifts to smaller H_{dc} and its width is getting smaller. In Figs. 5(b) and 5(c), similarly as in Fig. 3(b), each point is obtained for an independently constructed disordered lattice. Solid lines correspond to the 10th-order polynomials fitted to the numerical results. For the case $\Lambda=0.1$ in Fig. 5(c), where the statistical fluctuations due to disorder are relatively large we also show our estimate for the error bars [similarly as in Fig. 3(b)]. An example of the experimental results for a $Tl_2Ba_2Ca_2Cu_3O_{10}$ ceramic sample[32] is given in part (d) of Fig. 5. Here, the position of the maximum of the second harmonic has approximately the same value as the amplitude of the external field H_{ac}, similarly to the results of our calculations in the case $\Lambda=0.4$, see Fig. 5(c).

Up to now we concentrated on calculations and measurements corresponding to the temperature value well below the superconducting transition T_c of the grains. Increasing temperature destroys superconductivity of the grains and thus diminishes the critical current I_0 through a single junction from its maximal value at $T=0$ to zero at $T=T_c$. The functional form of $I_0(T)$ depends on the type of the junction, and is different for proximity[33,34] and tunnel[35] junctions. At the same time thermal fluctuations of normal currents and of the superconducting order parameter increase with temperature and lead to thermally activated flux creep. The characteristic time scale of flux-creep experiments[36] except in a narrow vicinity of T_c is of the order of 10^3 s which is much longer than the time scale in ac-susceptibility measurements, typically performed at frequencies 0.1–100 kHz.[12,22–24,32] We therefore expect that thermally activated processes do not play an important role in ac measurements performed at frequencies of that order, and the main temperature dependence of the susceptibilities should originate from the temperature-dependent parameter $\beta_0(T)$. The relative unimportance of thermal fluctuations with respect to the shape of the hysteresis loops has been confirmed by preliminary calculations, where thermal noise terms have been added to the right-hand side of Eqs. (2) and (3), and as a consequence, also to Eqs. (8)–(11). A more detailed study of thermal fluctuations and the associated time scales in flux-creep processes will be the subject of a forthcoming publication.

Since in ceramics tunneling junctions between neighboring grains determine the bulk properties of the sample[36] the parametrization of $\beta_0(T)$ may be taken as

$$\beta_0(T)=\beta_0(0)\sqrt{1-T/T_c}\,\tanh(1.54T_c\sqrt{1-T/T_c}/T)\ , \qquad (17)$$

where we substituted the general form of $\Delta(T)$ (Δ being the superconducting gap parameter) as given by the BCS theory[30] into the Ambegaokar-Baratoff[35] formula for $I_0(T)$ and assumed the self-inductance parameter L to be temperature independent. The first and second harmonics of magnetization as a function of temperature are displayed in Figs. 6(a) and 6(b). The data correspond to the H_{ac} field well above the critical field H_{c1} for this system and are very similar to the results of low-field–low ac-frequency measurements on sintered samples,[32] which *a posteriori* supports our assumptions concerning the role of thermally activated processes in this case. In crystallites and single crystals different types of weak links can be formed between coherent superconducting domains that are smaller in size than in the case of ceramics. It is therefore difficult to find the proper form of the "effective" $\beta_0(T)$. Due to substantially higher magnetic

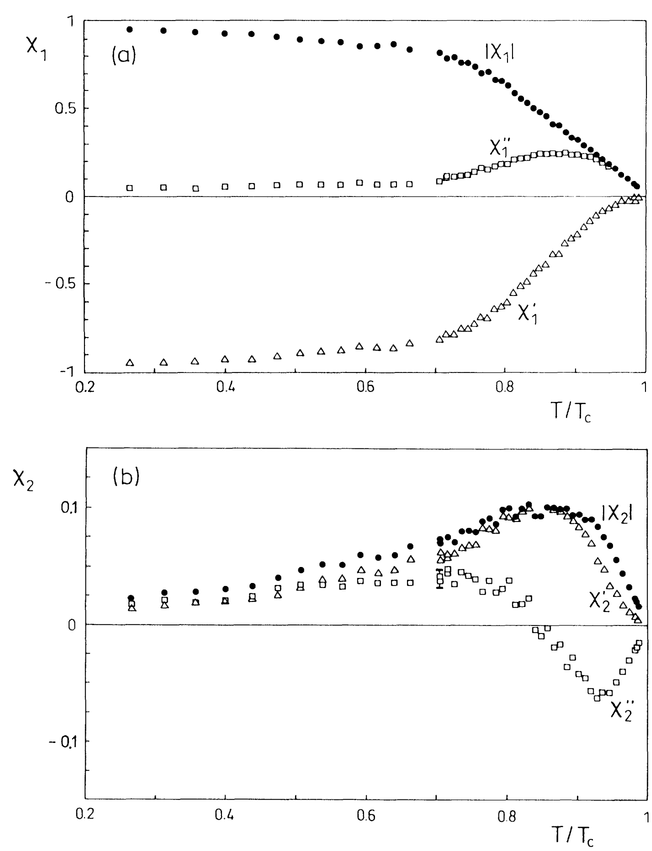

FIG. 6. (a) χ_1 and (b) χ_2 as function of temperature computed for a positionally disordered system of 10×10 junctions with $\beta_0(T)$ given by Eq. (17) with $\beta_0(0)=5$; other parameters are $\Lambda=0.4$, $H_{dc}=5\phi_0/a^2$, $H_{ac}=10\phi_0/a^2$, and $\omega=2\pi\times10^{-3}R/L$. Solid circles correspond to absolute values, triangles to the real parts, and squares to the imaginary parts of χ_1 and χ_2. Each point represents the result for one independently constructed disordered lattice.

fields that are of interest there and smaller domain sizes we expect fluctuations to play an important role in a much wider range of temperatures below T_c.

We conclude this section with rough estimates of the values of the characteristic parameters of the model corresponding to the actual high-T_c materials. Taking the data on ceramics and single crystals from Refs. 37 and 38, respectively, we get $\beta_0(0)=0.5-30$ for ceramics and $\beta_0(0)\sim 0.05$ for single crystals. The "natural" time unit in the model [cf. Eqs. (8)–(11)] $\tau=L/R\sim 10^{-12}$ s for sintered samples is to be compared with 10^{-3} s as a typical period of the ac field and 10^3 s—a characteristic time scale for thermally activated processes.[36] As a rough estimate of the corresponding magnetic inductance B we take one flux quantum ϕ_0 per one lattice mesh. This gives $B=10^{-4}-10^{-3}$ T for ceramics with grains some micrometers in diameter, and $B=0.1-1$ T for crystallites, if we assume that domains of coherent-order parameter values extend to distances not larger than a few coherence lengths (i.e., 10–30 Å). These values correspond very well with the critical fields measured for the materials in question. In summary, we considered a network of Josephson junctions with self-inductance effects as a model of strongly inhomogeneous superconductors. Self-inductances allowed us to describe local magnetic fields in a self-consistent manner. Within this model we were able to qualitatively reproduce ac susceptibilities of superconducting samples. We calculate higher harmonics of magnetization and discuss the role of disorder. In the case of ceramic samples our model is also quantitatively not far from the experimental results. We expect that with further extensions allowing us to account also for thermally activated processes (e.g., in the way it has been done for a loop with one junction in Ref. 39) this model will help us to understand the nature of the superconducting state in high-T_c materials on the mesoscopic scale.

ACKNOWLEDGMENTS

We thank Professor W. Dieterich for many valuable comments which helped to improve the text. We are very grateful for Ch. Heinzel, Ch. Neumann, Th. Ritzi, and P. Ziemann for allowing us access to their experimental data prior to publication and for many stimulating discussions. We profited a lot from many discussions with P. Brüll and P. Leiderer. This work was partly supported by the Polish State Committee for Scientific Research, Grant No. 2 0343 91 01 and by the Deutsche Forschungsgemeinschaft Grant No. SFB 306.

[1] K. A. Müller, M. Takashige, and J. G. Bednorz, Phys. Rev. Lett. **58**, 1143 (1987).
[2] I. Morgenstern, K. A. Müller, and J. G. Bednorz, Z. Phys. B **69**, 33 (1987).
[3] V. L. Aksenov and S. A. Sergeenkov, Physica C **156**, 18 (1988); **156**, 235 (1988).
[4] A. Majhofer, L. Mankiewicz, and J. Skalski, Phys. Rev. B **39**, 4334 (1989); **42**, 1022 (1990).
[5] David A. Huse and H. Sebastian Seung, Phys. Rev. B **42**, 1059 (1990).
[6] J. D. Reger, T. A. Tokuyasu, A. P. Young, and Matthew P. A. Fisher, Phys. Rev. B **44**, 7147 (1991).
[7] Ying-Hong Li and S. Teitel, Phys. Rev. Lett. **66**, 3301 (1991).
[8] W. Xia and P. L. Leath, Phys. Rev. Lett. **63**, 1428 (1989); Phys. Rev. B **44**, 9619 (1991).
[9] J. S. Chung, K. H. Lee, and D. Stroud, Phys. Rev. B **40**, 6570 (1989).
[10] G. Deutscher and K. A. Müller, Phys. Rev. Lett. **59**, 1745 (1987).
[11] John R. Clem, Physica C **153-155**, 50 (1988); **162-164**, 1137 (1989).
[12] M. Tinkham and C. J. Lobb, in *Solid State Physics,* edited by H. Ehrenreich and D. Turnbull (Academic, San Diego, 1989), Vol. 42.
[13] K.-H. Müller, J. C. Mac Farlane, and R. Driver, Physica C **158**, 69 (1989); **158**, 366 (1989).
[14] L. Ji, R. H. Sohn, G. C. Spalding, C. J. Lobb, and M. Tinkham, Phys. Rev. B **40**, 10 936 (1989).
[15] C. Bean, Phys. Rev. Lett. **8**, 250 (1962).
[16] Y. B. Kim, C. F. Hempstead, and A. R. Strnad, Phys. Rev. Lett. **9**, 306 (1962).
[17] P. W. Anderson, Phys. Rev. Lett. **9**, 309 (1962).
[18] Y. Yeshurun and P. Malozemoff, Phys. Rev. Lett. **60**, 2202 (1988).
[19] A. Majhofer, T. Wolf, and W. Dieterich, Phys. Rev. B **44**, 9634 (1991).
[20] T. Ishida and H. Mazaki, J. Appl. Phys. **52**, 6798 (1981).
[21] T. Ishida and R. B. Goldfarb, Phys. Rev. B **41**, 8937 (1990).
[22] C. D. Jeffries, Q. H. Lam, Y. Kim, L. C. Bourne, and A. Zettl, Phys. Rev. B **37**, 9840 (1988).
[23] Q. H. Lam and C. D. Jeffries, Phys. Rev. B **39**, 4772 (1989).
[24] C. D. Jeffries, Q. H. Lam, Y. Kim, C. M. Kim, A. Zettl, and P. M. Klein, Phys. Rev. B **39**, 11 526 (1989).
[25] A. Barone and G. Paterno, *Physics and Applications of the Josephson Effect* (Wiley, New York, 1982).
[26] E. B. Sonin, Pis'ma Zh. Eksp. Teor. Fiz. **47**, 415 (1988) [JETP Lett. **47**, 496 (1988)].
[27] E. B. Sonin and A. K. Tagantsev, Zh. Eksp. Teor. Fiz. **95**, 994 (1989) [Sov. Phys. JETP **68**, 572 (1989)]; Supercond. Sci. Technol. **4**, 119 (1991).
[28] A. P. Malozemoff, L. Krusin-Elbaum, D. C. Cronmayer, Y. Yeshurun, and F. Holtzberg, Phys. Rev. B **38**, 6490 (1988).
[29] A. M. Campbell and F. J. Blunt, Physica C **172**, 253 (1990).
[30] M. Tinkham, *Introduction to Superconductivity* (McGraw-Hill, New York, 1975).
[31] T. Wolf and J. Reinhard (unpublished).
[32] Th. Ritzi, Ch. Heinzel, Ch. Neumann, and P. Ziemann, Appl. Phys. Lett. **60**, 2297 (1992); Ch. Heinzel, Ch. Neumann, and P. Ziemann (unpublished), and private communication.
[33] P. G. de Gennes, Rev. Mod. Phys. **36**, 225 (1964).
[34] K. K. Likharev, Rev. Mod. Phys. **51**, 101 (1979).
[35] V. Ambegaokar and A. Baratoff, Phys. Rev. Lett. **10**, 486 (1963); **11**, 104 (1963).
[36] A. C. Mota, A. Pollini, P. Visani, K. A. Müller, and J. G. Bednorz, Phys. Rev. B **36**, 4011 (1987).
[37] R. Marcon, R. Fastampa, and M. Giura, Phys. Rev. B **39**, 2796 (1989).
[38] A. Umezawa, G. W. Crabtree, J. Z. Liu, T. J. Moran, S. K. Malik, L. H. Nunez, W. L. Kwok, and C. H. Sowers, Phys. Rev. B **38**, 2843 (1988).
[39] Th. M. Nieuwenhuizen and J. Pankert, Europhys. Lett. **11**, 457 (1990).